Supplementary Material – Directing excited state dynamics via chemical substitution: a systematic study of π-donors and π-acceptors at a carbon-carbon double bond

Katherine R. Herperger,[†] Anja Röder,[‡,¶] Ryan J. MacDonell,[‡] Andrey E. Boguslavskiy,[†] Anders B. Skov,[§] Albert Stolow,[*,‡,†,‖,¶] and Michael S. Schuurman[*,‖,‡]

†*Department of Physics, University of Ottawa, Ottawa, Ontario, K1N 6N5, Canada*

‡*Department of Chemistry and Biomolecular Sciences, University of Ottawa, Ottawa, Ontario, K1N 6N5, Canada*

¶*NRC-uOttawa Joint Centre for Extreme Photonics, Ottawa, ON K1A 0R6 Canada*

§*Department of Chemistry, University of Copenhagen, Universitetsparken 5, DK-2100 Copenhagen Ø, Denmark*

‖*National Research Council Canada, 100 Sussex Dr., Ottawa, Ontario, K1A 0R6, Canada*

E-mail: astolow@uottawa.ca; michael.schuurman@nrc-cnrc.gc.ca

1 Potential Energy Surfaces

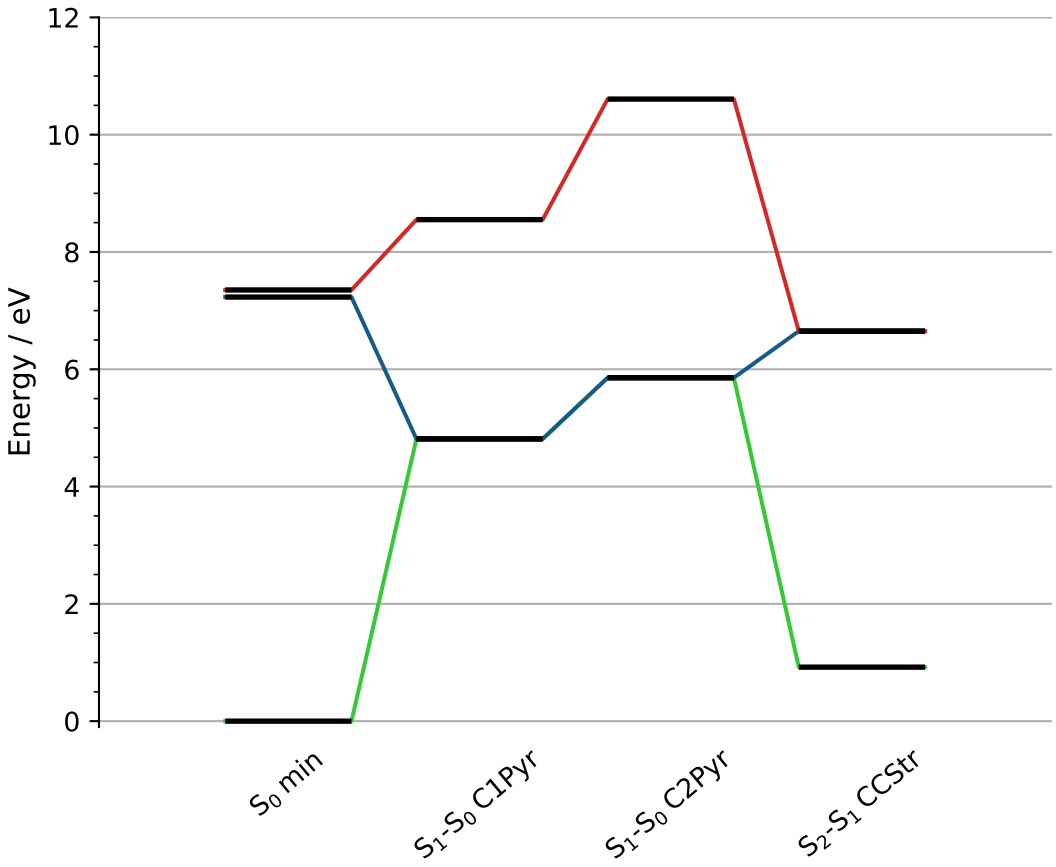

Figure S1: Minimum energy conical intersections of AN with respect to the optimized ground state geometry (S_0min).

Table S1: Potential energies of AN optimized geometries in Hartree.

	Energy / E_h		
Geometry	S_0	S_1	S_2
S_0min	−169.9759342	−169.7101914	−169.7057459
S_1-S_0 C1Pyr	−169.7990866	−169.7990791	−169.6616713
S_1-S_0 C2Pyr	−169.7607581	−169.7607577	−169.5861387
S_2-S_1 CCStr	−169.9420905	−169.7315311	−169.7315311

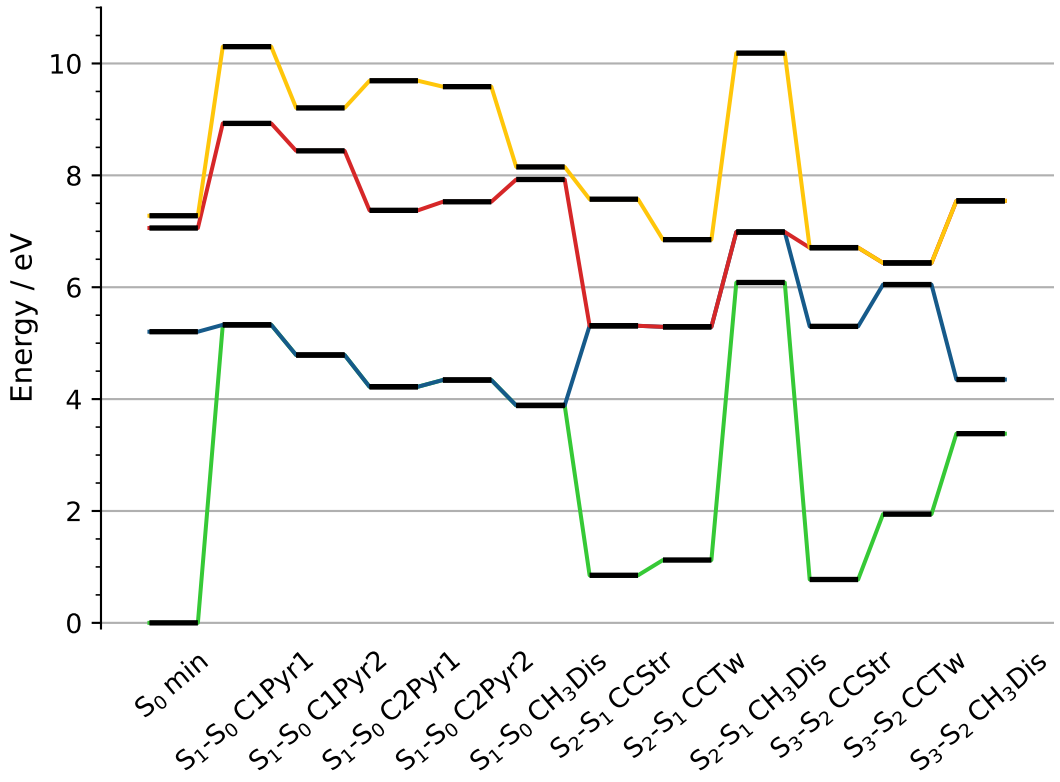

Figure S2: Minimum energy conical intersections of MVE with respect to the optimized ground state geometry (S_0min).

Table S2: Potential energies of MVE optimized geometries in Hartree.

	Energy / E_h			
Geometry	S_0	S_1	S_2	S_3
S_0min	−192.0481934	−191.8569282	−191.788801	−191.7807422
S_1-S_0 C1Pyr1	−191.8524219	−191.8524056	−191.7200724	−191.6696581
S_1-S_0 C1Pyr2	−191.8722341	−191.8722303	−191.7381032	−191.7099039
S_1-S_0 C2Pyr1	−191.8930652	−191.8930651	−191.7771845	−191.6920534
S_1-S_0 C2Pyr2	−191.8886565	−191.8886565	−191.7715650	−191.6959435
S_1-S_0 CH_3Dis	−191.9053776	−191.9053452	−191.7569118	−191.7486726
S_2-S_1 CCStr	−192.0169453	−191.8530347	−191.8530345	−191.7698718
S_2-S_1 CCTw	−192.0069158	−191.8537216	−191.8537211	−191.7964519
S_2-S_1 CH_3Dis	−191.8245908	−191.7914433	−191.7914136	−191.6739090
S_3-S_2 CCStr	−192.0197052	−191.8534083	−191.8017353	−191.8016818
S_3-S_2 CCTw	−191.9767731	−191.8259457	−191.8117487	−191.8117477
S_3-S_2 CH_3Dis	−191.9239035	−191.8883447	−191.7709566	−191.7709508

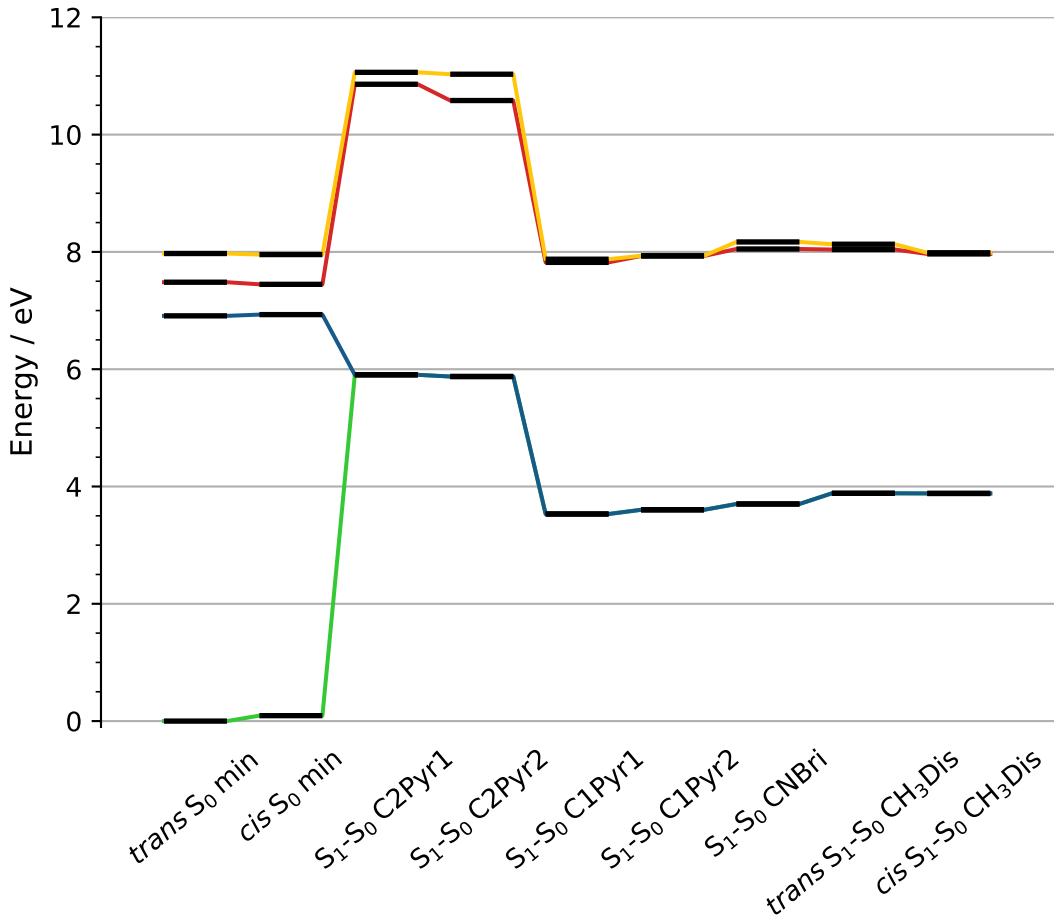

Figure S3: Minimum energy conical intersections of 1,2-MAN with respect to the optimized ground state geometry (S_0min).

Table S3: Potential energies of 1,2-MAN optimized geometries in Hartree.

	Energy / E_h			
Geometry	S_0	S_1	S_2	S_3
***trans* S_0min**	−283.9195447280	−283.6656240085	−283.6445384904	−283.6265542040
***cis* S_0min**	−283.9161444836	−283.6648395914	−283.6458606387	−283.6272178783
S_1-S_0 C1Pyr1	−283.7897799809	−283.7897759062	−283.6321032319	−283.6301274857
S_1-S_0 C1Pyr2	−283.7871588201	−283.7871570083	−283.6281099791	−283.6279735618
S_1-S_0 C2Pyr1	−283.7025681511	−283.7025679763	−283.5204942296	−283.5130272848
S_1-S_0 C2Pyr2	−283.7036292076	−283.7036254861	−283.5306914768	−283.5142070383
S_1-S_0 CNBri	−283.7835045109	−283.7835020461	−283.6237249524	−283.6193047247
***trans* S_1-S_0 CH_3Dis**	−283.7768253089	−283.7768177350	−283.6240614115	−283.6207321870
***cis* S_1-S_0 CH_3Dis**	−283.7768927479	−283.7768926265	−283.6268249640	−283.6260851842

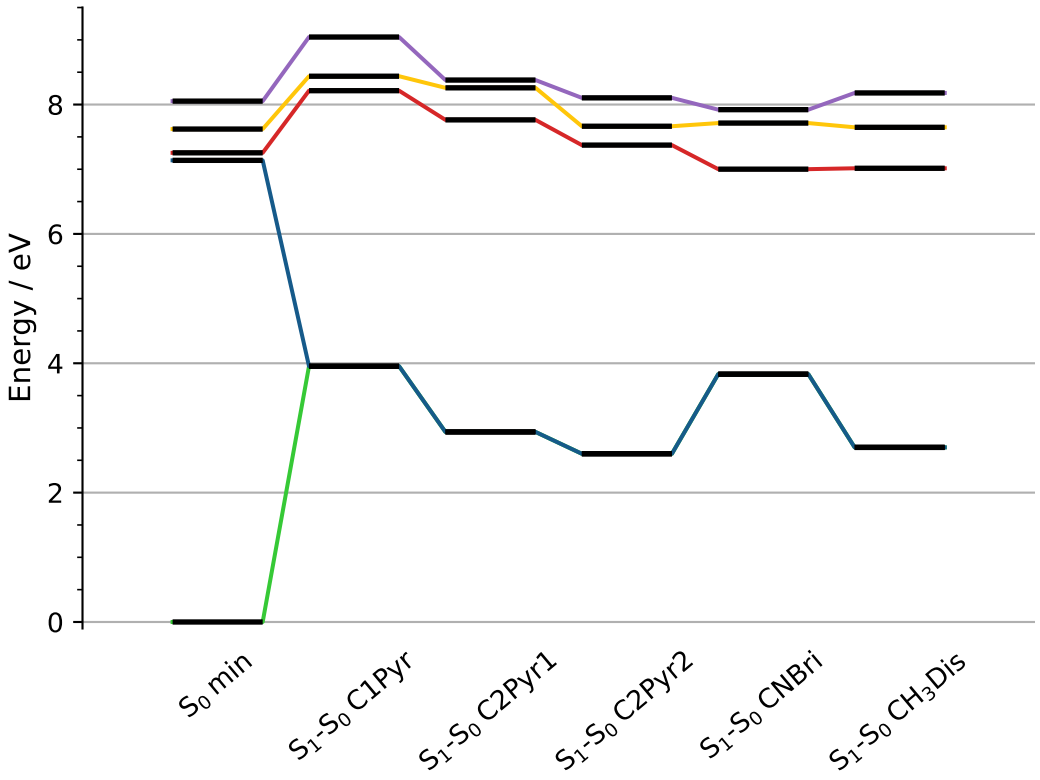

Figure S4: Minimum energy conical intersections of 1,1-MAN with respect to the optimized ground state geometry (S_0min).

Table S4: Potential energies of 1,1-MAN optimized geometries in Hartree.

Geometry	Energy / E_h		
	S_0	S_1	S_2
	S_3	S_4	
S_0min	−283.8602590835	−283.5979686143	−283.5936899515
	−283.5801968968	−283.5643256994	
S_1-S_0 C1Pyr	−283.7149393524	−283.7149304539	−283.5583953522
	−283.5501731788	−283.5279061937	
S_1-S_0 C2Pyr1	−283.7522760841	−283.7522719453	−283.5749731992
	−283.5567660401	−283.5523447855	
S_1-S_0 C2Pyr2	−283.7646747845	−283.7646728529	−283.5893087237
	−283.5785883543	−283.5624622350	
S_1-S_0 CNBri	−283.7194584089	−283.7194524312	−283.6029794575
	−283.5767878712	−283.5691722529	
S_1-S_0 CH_3Dis	−283.7610506077	−283.7610503964	−283.6024745155
	−283.5791972355	−283.5596700681	

2 Excited State Dynamics Simulations

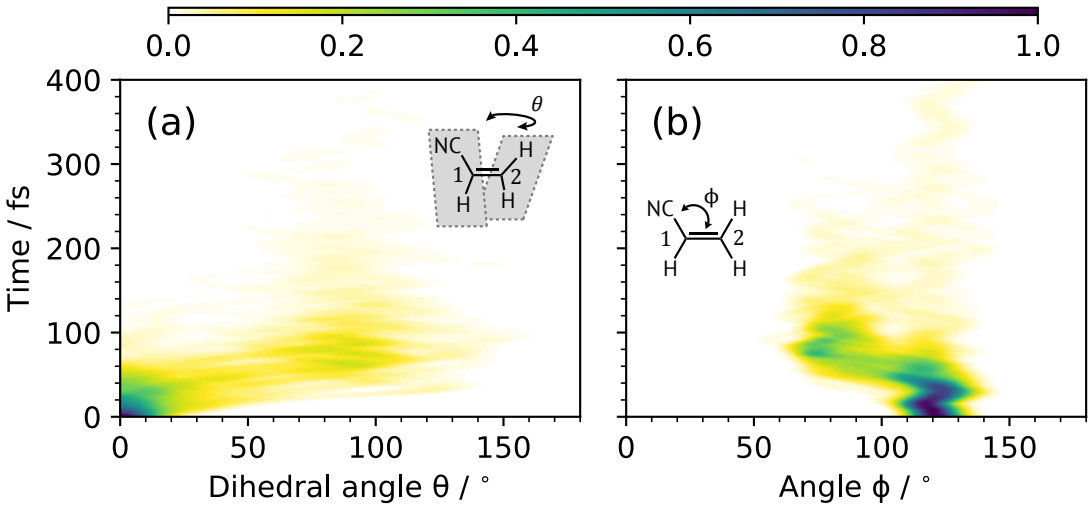

Figure S5: Normalized total excited state density of AN projected along (a) C=C torsion and (b) C=C−C bond angle. The weighted average of the total excited state density with the standard deviation is shown in the main text (Figure 5a,c).

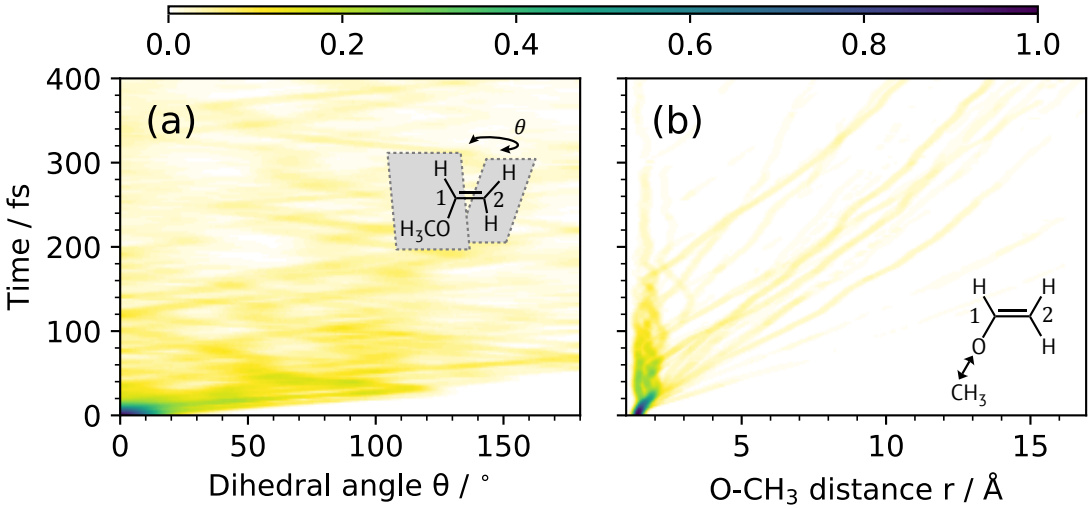

Figure S6: Normalized total excited state density of MVE projected along (a) C=C torsion and (b) O−CH_3 stretch. The weighted average of the total excited state density with the standard deviation is shown in the main text (Figure 5b,d).

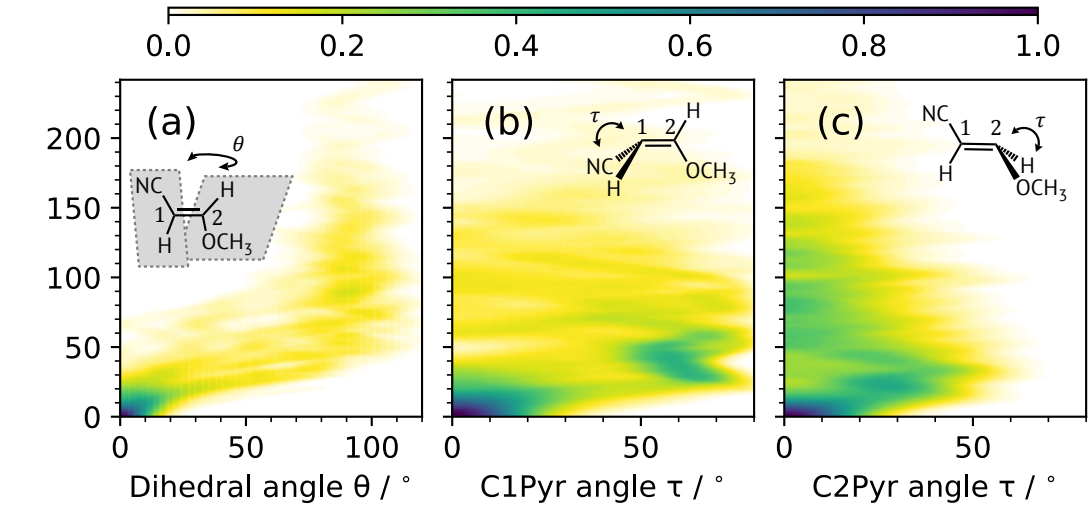

Figure S7: Normalized total excited state density of 1,2-MAN projected along (a) C=C torsion, (b) the C_1 pyramidalization angle, and (c) the C_2 pyramidalization angle. The weighted average of the total excited state density with the standard deviation is shown in the main text (Figure 6a,c,e).

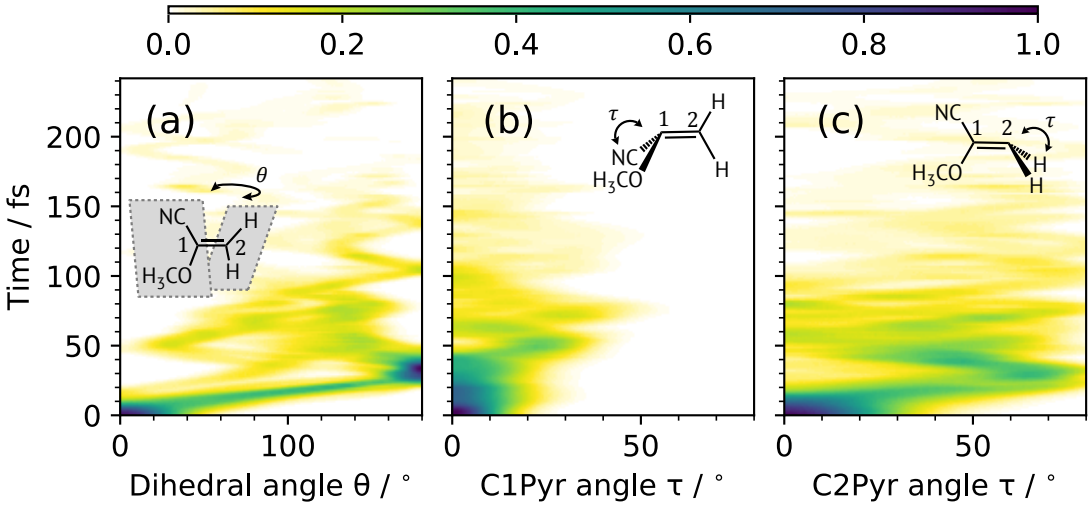

Figure S8: Normalized total excited state density of 1,1-MAN projected along (a) C=C torsion, (b) the C_1 pyramidalization angle, and (c) the C_2 pyramidalization angle. The weighted average of the total excited state density with the standard deviation is shown in the main text (Figure 6b,d,f).

3 Electronic Character

Table S5: Relative energy levels of each molecule's optimized ground state minimum geometry. Electronic character is shown for MR-CIS and ADC calculations. The excited state energies for a given electronic character are with respect to the S_0 energy. MCSCF and MR-CIS calculations: AN uses a 6-31G* basis set, MVE uses ANO(3s2p1d+3s(X), and the MAN isomers use ANO(3s2p1d). All ADC calculations were computed in a aug-cc-pVDZ basis. The oscillator strength is for transitions from the ground state, S_0, to an excited state, S_N, for the MR-CIS calculations.

	Electronic Character	**Energy / eV**				**Oscillator Strength**
		MCSCF	**MR-CIS**	**ADC(2)**	**ADC(3)**	$\mathbf{S_0 \rightarrow S_N}$
AN	$\pi_{CN}\pi^*$	7.54	7.23	7.31	6.74	0.0000
	$\pi\pi^*$	7.85	7.35	6.95	6.59	0.2773
	—	8.64	—	—	—	—
	—	9.14	—	—	—	—
MVE	π3s	5.21	5.20	5.77	6.10	0.0424
	π3p	7.11	7.06	6.19	6.50	0.0061
	$\pi\pi^*$	8.34	7.28	6.62	6.86	0.3679
	—	8.93	8.97	6.62	6.88	0.0119
	—	10.40	—	6.93	7.31	—
	—	11.16	—	7.09	—	—
***trans*-1,2-MAN**	$\pi\pi^*$	7.71	6.87	6.20	6.11	0.4321
	$\pi_{CN}\pi^*$	7.86	7.47	7.78	7.29	0.0000
	$\pi\pi^*_{CN}$	8.99	7.96	7.34	7.04	0.0002
***cis*-1,2-MAN**	$\pi\pi^*$	7.56	6.85	6.02	5.97	0.3828
	$\pi_{CN}\pi^*$	7.70	7.25	7.48	7.09	0.0003
	$\pi\pi^*_{CN}$	8.24	7.64	7.32	6.76	0.0008
1,1-MAN	$\pi\pi^*$	7.63	6.81	6.21	6.37	0.3897
	$\pi\pi^*_{CN}$	7.70	7.25	7.57	6.72	0.0003
	π3s	8.25	7.63	6.29	6.56	0.0007
	$\pi_{CN}\pi^*$	8.74	8.17	7.97	7.32	0.0483

4 Conical Intersection Analysis

Iterative Hirshfeld charges for the MECIs marked with red symbols used in Figure 7.

Table S6: AN: iterative Hirshfeld charges.

	CNBri	**C1Pyr**	**C2Pyr**
C(1)	−0.58	−0.56	0.16
C(2)	0.23	0.18	−0.60
C(3)	0.31	0.32	0.25
N(4)	−0.34	−0.40	−0.26
H(5)	0.19	0.25	0.09
H(6)	0.10	0.12	0.12
H(7)	0.09	0.09	0.25

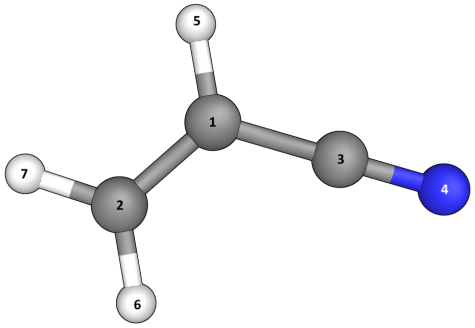

Table S7: MVE: iterative Hirshfeld charges.

	C1Pyr	**C2Pyr**	**CH_3Dis**
C(1)	−0.52	0.74	0.38
C(2)	0.14	−0.98	−0.27
C(3)	−0.10	−0.02	−0.35
O(4)	−0.03	−0.35	−0.36
H(5)	0.07	0.15	0.16
H(6)	0.09	0.16	0.13
H(7)	0.09	0.01	0.02
H(8)	0.10	0.11	0.08
H(9)	0.09	0.11	0.08
H(10)	0.07	0.09	0.11

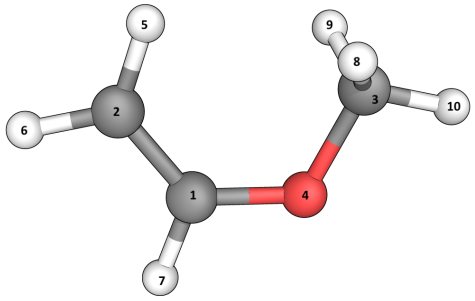

Table S8: 1,2-MAN: iterative Hirshfeld charges. While the *trans* CH_3Dis MECI is used in Figure 7, the *cis* CH_3Dis MECI values are included here for comparison.

	CNBri	**C1Pyr1**	**C2Pyr2**	***trans (cis)* CH_3Dis**
C(1)	−0.80	−0.64	0.23	−0.51 (−0.45)
C(2)	0.69	0.58	−0.40	0.42 (0.47)
C(3)	0.35	0.34	0.19	0.32 (0.34)
C(4)	−0.04	−0.04	−0.05	0.03 (−0.02)
O(5)	−0.30	−0.31	−0.16	−0.52 (−0.53)
N(6)	−0.50	-0.48	−0.28	−0.46 (−0.44)
H(7)	0.11	0.11	0.08	0.18 (0.15)
H(8)	0.12	0.11	0.08	0.18 (0.16)
H(9)	0.13	0.11	0.10	0.18 (0.15)
H(10)	0.05	0.06	0.10	0.06 (0.04)
H(11)	0.20	0.15	0.12	0.10 (0.14)

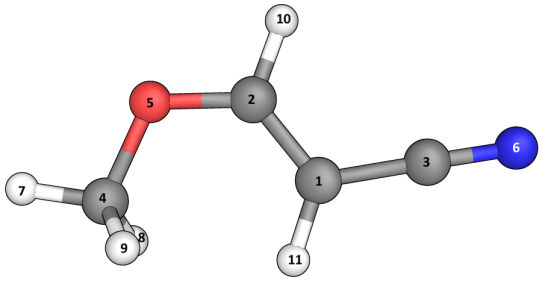

Table S9: 1,1-MAN: iterative Hirshfeld charges.

	CNBri	**C1Pyr**	**C2Pyr2**	**CH_3Dis**
C(1)	0.03	−0.38	0.68	0.50
C(2)	0.04	0.27	−0.76	−0.44
C(3)	0.20	0.27	0.10	0.18
C(4)	0.01	−0.04	−0.01	−0.10
O(5)	−0.36	−0.16	−0.36	−0.51
N(6)	−0.33	−0.44	−0.26	−0.32
H(7)	0.08	0.07	0.10	0.15
H(8)	0.06	0.10	0.11	0.14
H(9)	0.05	0.08	0.11	0.13
H(10)	0.11	0.12	0.12	0.14
H(11)	0.11	0.11	0.17	0.13

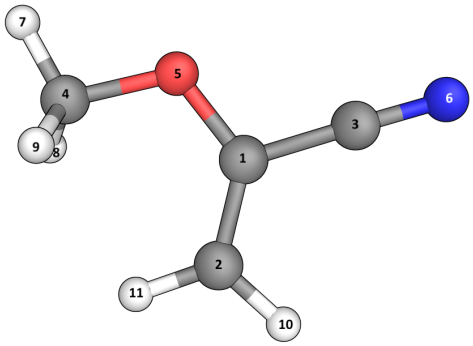

5 Molecular Geometries

The following geometries are in units of Ångströms.

Table S10: MR-CIS(6,6)/6-31G* optimized geometry of AN S_0 minimum (**S_0min**).

C	−0.693738	0.510927	0.000000
C	−1.707824	−0.381287	0.000000
C	0.682629	0.110948	0.000000
N	1.811068	−0.214787	0.000000
H	−0.879238	1.569931	0.000000
H	−1.525754	−1.441619	0.000000
H	−2.729162	−0.045861	0.000000

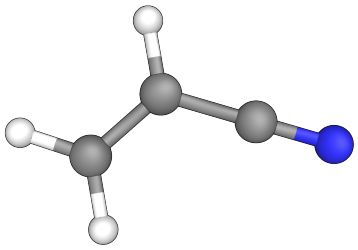

Table S11: MR-CIS(6,6)/6-31G* optimized geometry of AN S_1-S_0 C1 bridging MECI (**CNBri**).

C	−0.692138	0.725680	0.244029
C	−1.491540	−0.397464	−0.232835
C	0.294724	−0.014657	−0.338793
N	0.839692	−0.987668	−0.830813
H	−0.844667	1.778325	0.311097
H	−1.787047	−1.192203	0.437892
H	−1.772662	−0.534213	−1.268346

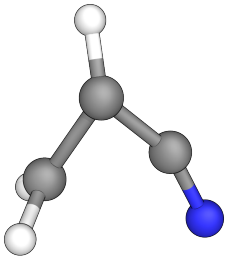

Table S12: MR-CIS(6,6)/6-31G* optimized geometry of AN S_1-S_0 C1 pyramidalizing MECI (**C1Pyr**).

C	−0.701776	0.604814	−0.154219
C	−1.680407	−0.391471	0.017255
C	−0.708484	1.764333	−0.933030
N	−0.587437	2.752587	−1.571293
H	−1.304842	0.929554	0.798397
H	−1.390297	−1.372762	0.362662
H	−2.748778	−0.202406	0.016718

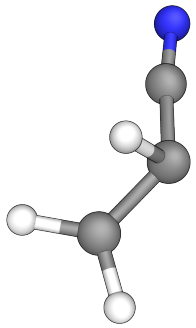

Table S13: MR-CIS(6,6)/6-31G* optimized geometry of AN S_1-S_0 C2 pyramidalizing MECI (**C2Pyr**).

C	−0.748496	−3.157676	−0.788411
C	−1.627841	−2.059672	−0.822326
C	0.513430	−3.082754	−1.467357
N	1.528629	−3.037786	−2.054121
H	−0.951497	−4.145892	−0.382845
H	−2.419967	−2.027722	−0.079428
H	−2.117721	−2.967584	−1.431211

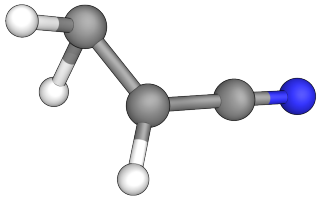

Table S14: MR-CIS(6,6)/6-31G* optimized geometry of AN S_2-S_1 CC stretching MECI (**CCStr**).

C	−0.649959	0.634697	0.026347
C	−1.706339	−0.414488	−0.002033
C	0.604329	0.107718	−0.060571
N	1.694962	−0.513850	−0.146036
H	−0.852007	1.681352	0.101487
H	−1.416541	−1.446558	−0.082445
H	−2.751985	−0.173384	0.057251

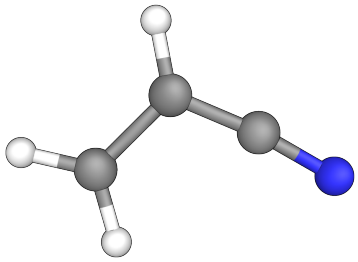

Table S15: MR-CIS(4,5)/ANO(3s2p1d+3s(X)) optimized geometry of MVE S_0 minimum (**S_0min**).

C	−0.717033	−0.557294	0.000000
C	−1.506366	0.560417	0.000000
C	1.375895	0.610393	0.000000
O	0.623729	−0.636905	0.000000
H	−1.116762	1.565401	0.000000
H	−2.577457	0.423078	0.000000
H	−1.158145	−1.545326	0.000000
H	1.137131	1.172770	0.896057
H	1.137130	1.172771	−0.896056
H	2.419644	0.317264	−0.000001

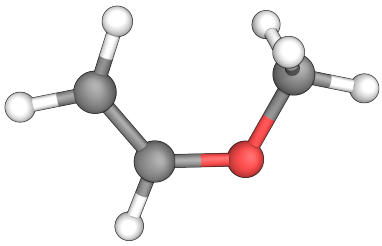

Table S16: MR-CIS(4,5)/ANO(3s2p1d+3s(X)) optimized geometry of MVE S_1-S_0 C1 pyramidalizing MECI 1 (**C1Pyr1**).

C	−0.590260	−0.001798	0.123179
C	−1.902746	0.577982	−0.095597
C	1.699377	0.394780	0.108748
O	0.527187	0.154658	−0.639119
H	−2.405566	0.608768	−1.066096
H	−2.554324	0.633080	0.771870
H	−1.204197	−0.865207	−0.596760
H	1.935343	−0.462494	0.736372
H	1.580194	1.279493	0.733614
H	2.496588	0.557210	−0.613145

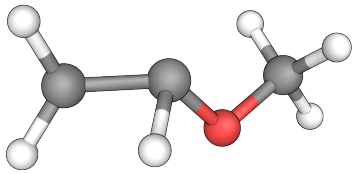

Table S17: MR-CIS(4,5)/ANO(3s2p1d+3s(X)) optimized geometry of MVE S_1-S_0 C1 pyramidalizing MECI 2 (**C1Pyr2**).

C	−0.681785	−0.075155	0.206538
C	−1.989721	0.468766	−0.162581
C	0.299173	2.197814	−0.305610
O	−0.202132	0.985580	−0.866331
H	−2.495932	0.182839	−1.082938
H	−2.429521	1.282823	0.401677
H	−0.436820	−1.041340	−0.219559
H	1.376418	2.090191	−0.209552
H	−0.133007	2.374992	0.674111
H	0.053591	3.012885	−0.983229

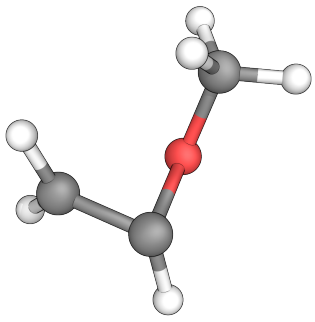

Table S18: MR-CIS(4,5)/ANO(3s2p1d+3s(X)) optimized geometry of MVE S_1-S_0 C2 pyramidalizing MECI 1 (**C2Pyr1**).

C	−0.690656	−0.598618	−0.003075
C	−1.496961	0.591929	0.051831
C	1.350432	0.600954	0.002041
O	0.611302	−0.617986	−0.026289
H	−2.157236	0.617998	−0.828048
H	−2.126278	0.556972	0.953823
H	−1.052876	−1.658030	−0.032694
H	1.135586	1.150771	0.911770
H	1.098858	1.214451	−0.855941
H	2.391098	0.294800	−0.031138

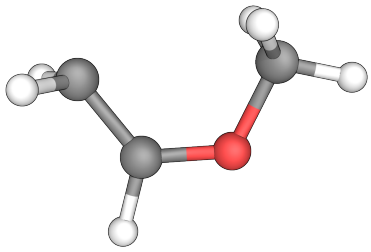

Table S19: MR-CIS(4,5)/ANO(3s2p1d+3s(X)) optimized geometry of MVE S_1-S_0 C2 pyramidalizing MECI 2 (**C2Pyr2**).

C	−0.716904	−0.601862	0.011119
C	−1.611873	0.523076	−0.052855
C	1.321274	0.604009	−0.008125
O	0.587287	−0.613277	0.032950
H	−1.424935	1.185667	0.813751
H	−1.395590	1.107289	−0.967707
H	−1.053193	−1.647828	0.051284
H	1.072021	1.220878	0.848577
H	1.102393	1.142686	−0.923850
H	2.364151	0.308913	0.022751

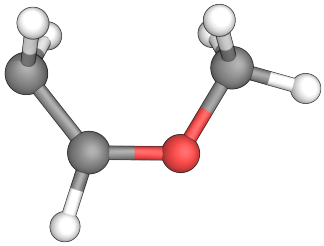

Table S20: MR-CIS(4,5)/ANO(3s2p1d+3s(X)) optimized geometry of MVE S_1-S_0 dissociating MECI (**CH_3Dis**).

C	−0.795116	−0.671540	0.000027
C	−1.517121	0.529440	−0.000014
C	1.733144	1.101768	0.000012
O	0.426573	−0.831212	−0.000061
H	−1.081140	1.518050	0.000017
H	−2.595096	0.444001	0.000001
H	−1.373788	−1.592207	−0.000059
H	1.205044	1.293621	0.923969
H	1.205107	1.293631	−0.924000
H	2.422536	0.270686	−0.000022

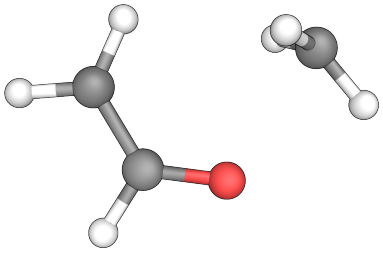

Table S21: MR-CIS(4,5)/ANO(3s2p1d+3s(X)) optimized geometry of MVE S_2-S_1 stretching MECI (**CCStr**).

C	−0.736791	−0.570205	−0.001743
C	−1.626696	0.543868	0.003450
C	1.520638	0.703842	−0.001679
O	0.544797	−0.631690	−0.001059
H	−1.347606	1.572921	−0.006803
H	−2.687974	0.297164	0.016707
H	−1.202262	−1.529489	0.001151
H	1.187335	1.150221	0.944803
H	1.203667	1.128387	−0.964927
H	2.436216	0.101514	0.014933

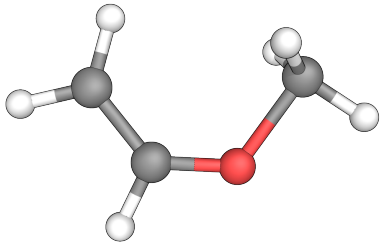

Table S22: MR-CIS(4,5)/ANO(3s2p1d+3s(X)) optimized geometry of MVE S_2-S_1 twisting MECI (**CCTw**).

C	−0.737020	−0.603792	−0.060519
C	−1.599045	0.545841	0.052000
C	1.465264	0.717623	0.019640
O	0.536480	−0.645596	−0.046350
H	−1.411283	1.492409	−0.414295
H	−2.557648	0.382420	0.539405
H	−1.201253	−1.575156	0.018970
H	1.012638	1.366942	0.751365
H	1.426807	1.054479	−1.011362
H	2.387052	0.244211	0.330784

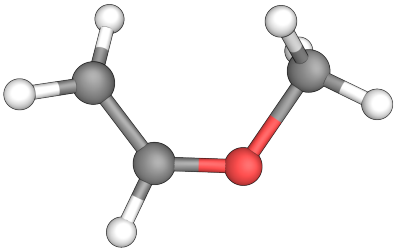

Table S23: MR-CIS(4,5)/ANO(3s2p1d+3s(X)) optimized geometry of MVE S_2-S_1 dissociating MECI (**CH_3Dis**).

C	−0.975705	−0.838858	0.066501
C	−1.502800	0.415244	−0.039137
C	1.709729	1.051466	0.000796
O	0.322458	−0.298890	0.060066
H	−0.672590	1.145037	−0.075793
H	−2.475816	0.839063	−0.113907
H	−1.341215	−1.844632	0.152976
H	1.224353	1.404626	0.903822
H	1.238444	1.399315	−0.915935
H	2.514557	0.354756	0.000467

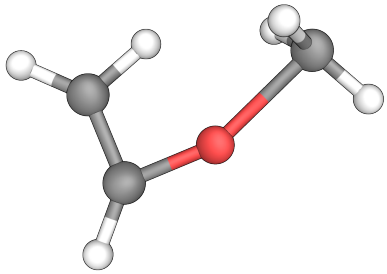

Table S24: MR-CIS(4,5)/ANO(3s2p1d+3s(X)) optimized geometry of MVE S_3-S_2 stretching MECI (**CCStr**).

C	−0.712303	−0.688867	−0.000296
C	−1.542581	0.612557	0.000506
C	1.368372	0.655874	−0.000292
O	0.600325	−0.649426	−0.000027
H	−1.058294	1.572164	0.001179
H	−2.616747	0.523329	0.000670
H	−1.124039	−1.685240	−0.000833
H	1.109606	1.196784	0.898115
H	1.113657	1.193836	−0.901860
H	2.400014	0.329373	0.002478

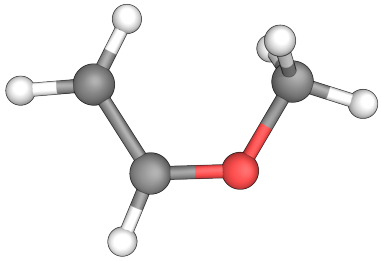

Table S25: MR-CIS(4,5)/ANO(3s2p1d+3s(X)) optimized geometry of MVE S_3-S_2 twisting MECI (**CCTw**).

C	−0.770706	−0.694710	0.065614
C	−1.553089	0.578546	−0.079278
C	1.398850	0.698718	0.010857
O	0.519185	−0.652111	0.183948
H	−1.136792	1.375955	−0.669533
H	−2.591551	0.599084	0.213392
H	−1.151862	−1.650104	−0.286533
H	1.586899	0.875391	1.060730
H	0.764417	1.445769	−0.437298
H	2.309523	0.491117	−0.542236

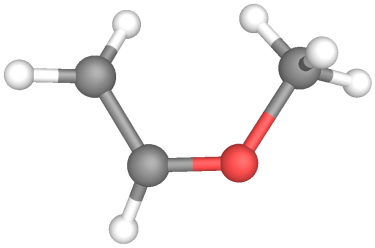

Table S26: MR-CIS(4,5)/ANO(3s2p1d+3s(X)) optimized geometry of MVE S_3-S_2 dissociating MECI (**CH_3Dis**).

C	−0.837163	−0.681723	0.000006
C	−1.520544	0.500170	−0.000009
C	1.690578	1.050659	−0.000007
O	0.439992	−0.644346	0.000008
H	−0.980815	1.435313	0.000006
H	−2.597324	0.518657	0.000021
H	−1.325752	−1.650019	−0.000017
H	1.284363	1.422960	0.933501
H	1.284402	1.422995	−0.933509
H	2.547954	0.395374	0.000019

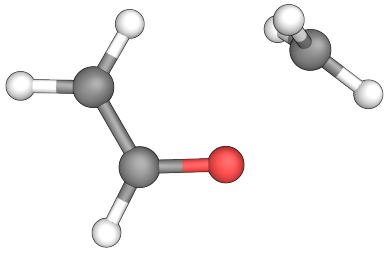

Table S27: MR-CIS(6,6)/ANO(3s2p1d) optimized geometry of 1,2-MAN S_0 *trans* minimum (***trans* S_0min**).

C	0.428447	−0.409887	0.000000
C	−0.429883	0.650695	0.000000
C	1.853005	−0.169684	0.000000
C	−2.370207	−0.682151	0.000000
O	−1.776984	0.620271	0.000000
N	3.018735	0.015798	0.000000
H	−3.458750	−0.519883	0.000000
H	−2.074223	−1.248976	−0.904130
H	−2.074223	−1.248976	0.904130
H	−0.055925	1.682189	0.000000
H	0.097137	−1.452595	0.000000

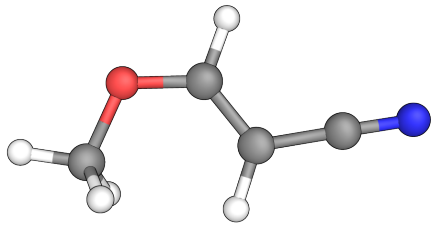

Table S28: MR-CIS(6,6)/ANO(3s2p1d) optimized geometry of 1,2-MAN S_0 *cis* minimum (***cis* S_0min**).

C	0.427767	−1.163366	0.000000
C	−0.929967	−1.010978	0.000000
C	1.448168	−0.141094	0.000000
C	−1.075189	1.367861	0.000000
O	−1.715046	0.080407	0.000000
N	2.325456	0.649278	0.000000
H	−1.895774	2.101776	0.000000
H	−0.451822	1.498419	−0.902751
H	−0.451822	1.498419	0.902751
H	−1.548642	−1.917519	0.000000
H	0.795005	−2.195882	0.000000

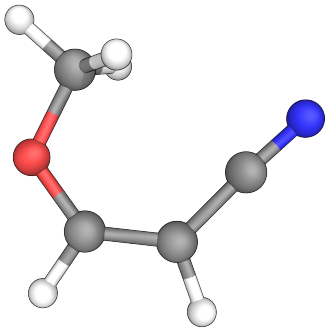

Table S29: MR-CIS(6,6)/ANO(3s2p1d) optimized geometry of 1,2-MAN S_1-S_0 C1 pyramidalizing MECI 1 (**C1Pyr1**).

C	0.432619	−0.414094	−0.040901
C	−0.491436	0.697963	−0.009195
C	1.690584	0.030746	−0.527635
C	−0.523305	0.789391	2.352402
O	−0.935494	1.250306	1.046389
N	2.747645	0.464671	−0.844941
H	−1.057306	1.430474	3.043556
H	−0.803486	−0.249510	2.475088
H	0.549224	0.904120	2.449075
H	−0.886468	1.207523	−0.894511
H	0.037401	−1.318251	−0.498051

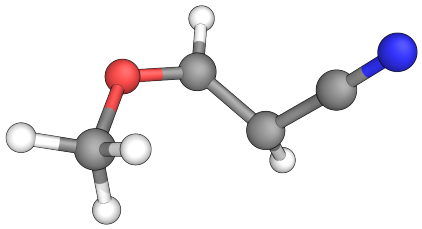

Table S30: MR-CIS(6,6)/ANO(3s2p1d) optimized geometry of 1,2-MAN S_1-S_0 C1 pyramidalizing MECI 2 (**C1Pyr2**).

C	0.512712	−0.442914	−0.001663
C	−0.424484	0.656703	−0.040453
C	1.780197	−0.038270	−0.491917
C	−0.580720	0.816165	−2.397439
O	−0.932302	1.221611	−1.053431
N	2.841476	0.355317	−0.846863
H	−1.198477	1.435208	−3.035808
H	0.473918	1.002728	−2.554224
H	−0.807316	−0.234927	−2.526652
H	−0.795418	1.142502	0.867948
H	0.123521	−1.378966	−0.394013

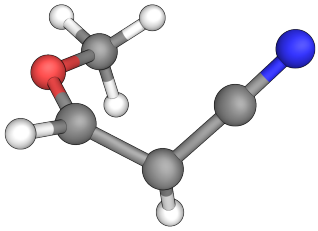

Table S31: MR-CIS(6,6)/ANO(3s2p1d) optimized geometry of 1,2-MAN S_1-S_0 C2 pyramidalizing MECI 1 (**C2Pyr1**).

C	0.351764	−0.433969	−0.039186
C	−0.530669	0.733849	−0.150092
C	1.706061	−0.287122	0.383216
C	−0.408820	0.915666	2.302315
O	−0.826458	0.132599	1.195063
N	2.825850	−0.170250	0.728963
H	−0.518966	0.296169	3.189628
H	0.623004	1.235214	2.191866
H	−1.051274	1.791320	2.356935
H	−1.405053	0.535194	−0.765767
H	0.038666	−1.456400	−0.242100

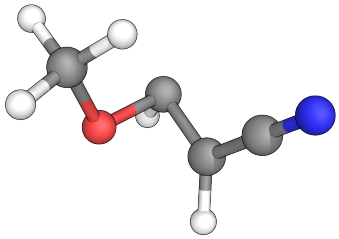

Table S32: MR-CIS(6,6)/ANO(3s2p1d) optimized geometry of 1,2-MAN S_1-S_0 C2 pyramidalizing MECI 2 (**C2Pyr2**).

C	0.583697	−0.384554	−0.175197
C	−0.501100	0.582159	0.116740
C	1.947408	−0.147175	0.161200
C	−0.722502	0.763593	−2.313967
O	0.077503	1.039316	−1.174602
N	3.040253	0.017696	0.573102
H	−0.065134	0.751709	−3.180115
H	−1.234973	−0.188212	−2.203197
H	−1.461226	1.556837	−2.405971
H	−0.215461	1.329008	0.855760
H	0.376465	−1.302748	−0.710393

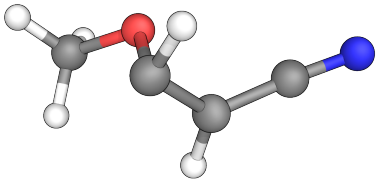

Table S33: MR-CIS(6,6)/ANO(3s2p1d) optimized geometry of 1,2-MAN S_1-S_0 CN bridging MECI (**CNBri**).

C	0.505819	−0.587124	0.048004
C	−0.543273	0.373931	0.019140
C	1.693862	0.136498	−0.066055
C	−0.488896	0.832574	2.333706
O	−1.008737	1.012602	0.977087
N	2.616442	0.886254	−0.166685
H	−1.117180	1.476689	2.935508
H	−0.579928	−0.207825	2.609725
H	0.545808	1.146834	2.333115
H	−1.044962	0.723348	−0.898677
H	0.364633	−1.635425	0.228657

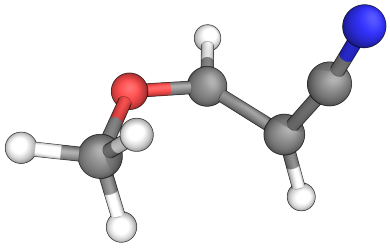

Table S34: MR-CIS(6,6)/ANO(3s2p1d) optimized geometry of 1,2-MAN S_1-S_0 *trans* CH_3 dissociating MECI (***trans* CH_3Dis**).

C	0.441087	−0.354955	0.001623
C	−0.420616	0.746298	0.000290
C	1.846024	−0.172791	−0.002732
C	−2.681849	−1.238308	0.012555
O	−1.653774	0.688007	0.003682
N	3.018389	−0.039276	−0.006429
H	−3.636470	−0.736607	0.012904
H	−2.292807	−1.622233	−0.918739
H	−2.288940	−1.615243	0.944850
H	0.039374	1.741443	−0.004099
H	0.056031	−1.362480	0.005986

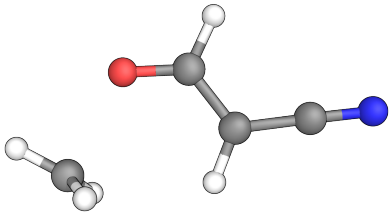

Table S35: MR-CIS(6,6)/ANO(3s2p1d) optimized geometry of 1,2-MAN S_1-S_0 *cis* dissociating MECI (***cis* CH_3Dis**).

C	0.420780	−1.289128	−0.001294
C	−0.970842	−1.104870	−0.002650
C	1.352712	−0.222668	−0.000512
C	−0.830619	2.052427	−0.009341
O	−1.592284	−0.041840	−0.004604
N	2.153359	0.644181	0.000631
H	−1.862591	2.366785	−0.011135
H	−0.281313	2.015442	−0.936953
H	−0.281846	2.023516	0.918884
H	−1.562539	−2.028247	−0.001620
H	0.815636	−2.295688	−0.000371

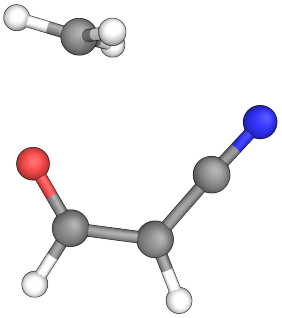

Table S36: MR-CIS(6,6)/ANO(3s2p1d) optimized geometry of 1,1-MAN S_0 minimum (**S_0min**).

C	0.004931	−0.292151	0.000000
C	−0.309431	−1.613843	0.000000
C	1.402492	0.133435	0.000000
C	−2.224547	0.458218	0.000000
O	−0.832996	0.782383	0.000000
N	2.535145	0.458918	0.000000
H	−2.756549	1.421837	0.000000
H	−2.497005	−0.121421	−0.903926
H	−2.497005	−0.121421	0.903926
H	0.502070	−2.347736	0.000000
H	−1.341743	−1.974970	0.000000

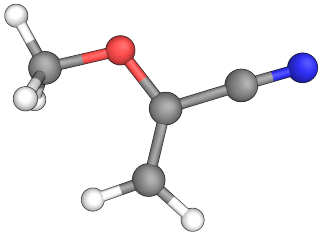

Table S37: MR-CIS(6,6)/ANO(3s2p1d) optimized geometry of 1,1-MAN S_1-S_0 C1 pyramidalizing MECI (**C1Pyr**).

C	−0.720066	0.703253	−0.053472
C	−1.711541	−0.372508	−0.082083
C	−0.768608	1.774058	−0.985076
C	−0.667429	0.706788	2.361596
O	−1.425671	0.968551	1.188467
N	−0.662464	2.646069	−1.777132
H	−0.126187	−0.231337	2.269014
H	0.040695	1.519928	2.503813
H	−1.371256	0.663517	3.189067
H	−1.455537	−1.356931	0.293968
H	−2.756519	−0.181575	−0.317200

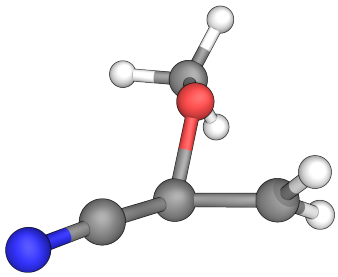

Table S38: MR-CIS(6,6)/ANO(3s2p1d) optimized geometry of 1,1-MAN S_1-S_0 C2 pyramidalizing MECI 1 (**C2Pyr1**).

C	−0.050448	−0.278908	0.028691
C	−0.243533	−1.678506	0.102850
C	1.333088	0.210139	−0.017059
C	−2.262172	0.530568	0.020760
O	−0.836661	0.726549	−0.010686
N	2.470794	0.511900	−0.050343
H	−2.674854	1.530778	−0.025156
H	−2.564090	−0.061141	−0.835011
H	−2.537435	0.031247	0.941909
H	−0.954183	−1.860335	−0.731590
H	−0.928496	−1.773358	0.972478

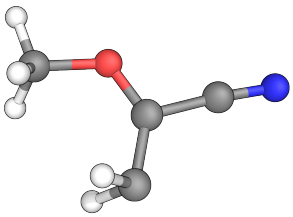

Table S39: MR-CIS(6,6)/ANO(3s2p1d) optimized geometry of 1,1-MAN S_1-S_0 C2 pyramidalizing MECI 2 (**C2Pyr2**).

C	−0.003616	−0.265522	0.002793
C	−0.348130	−1.644302	0.058407
C	1.377655	0.214631	−0.029385
C	−2.243476	0.474254	−0.004033
O	−0.813572	0.713788	−0.026141
N	2.545182	0.387750	−0.049917
H	−2.670684	1.469577	−0.042000
H	−2.521216	−0.120575	−0.863385
H	−2.506011	−0.046210	0.906896
H	0.204962	−2.091683	−0.787744
H	0.222026	−2.027306	0.924509

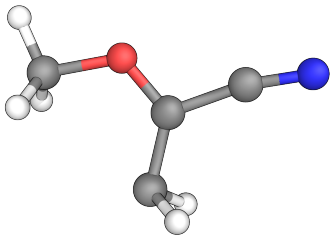

Table S40: MR-CIS(6,6)/ANO(3s2p1d) optimized geometry of 1,1-MAN S_1-S_0 CN bridging MECI (**CNBri**).

C	−0.009653	−0.563814	0.282864
C	−0.059309	−1.916663	−0.338742
C	−0.031625	−0.194418	−1.038479
C	0.064660	0.216492	2.467648
O	0.770769	−0.102268	1.290814
N	−0.275601	−0.481771	−2.208838
H	0.800522	0.569659	3.186354
H	−0.669957	0.998512	2.275951
H	−0.442216	−0.662976	2.868157
H	0.766550	−2.343135	−0.908504
H	−0.982379	−2.494935	−0.315491

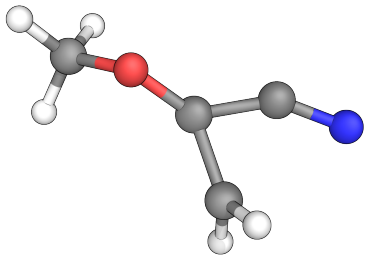

Table S41: MR-CIS(6,6)/ANO(3s2p1d) optimized geometry of 1,1-MAN S_1-S_0 dissociating MECI (**CH_3Dis**).

C	0.051473	−0.259181	0.002229
C	−0.262212	−1.610019	0.000985
C	1.474127	0.085097	−0.004526
C	−2.940131	0.344064	0.019029
O	−0.742138	0.694926	0.008179
N	2.613421	0.368239	−0.009987
H	−3.110386	1.409216	0.021668
H	−3.002917	−0.195902	−0.913968
H	−2.992610	−0.198871	0.950934
H	0.525720	−2.349812	−0.004653
H	−1.294125	−1.926618	0.005479

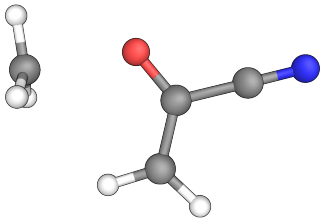

6 TRPES: Fit and Residuals

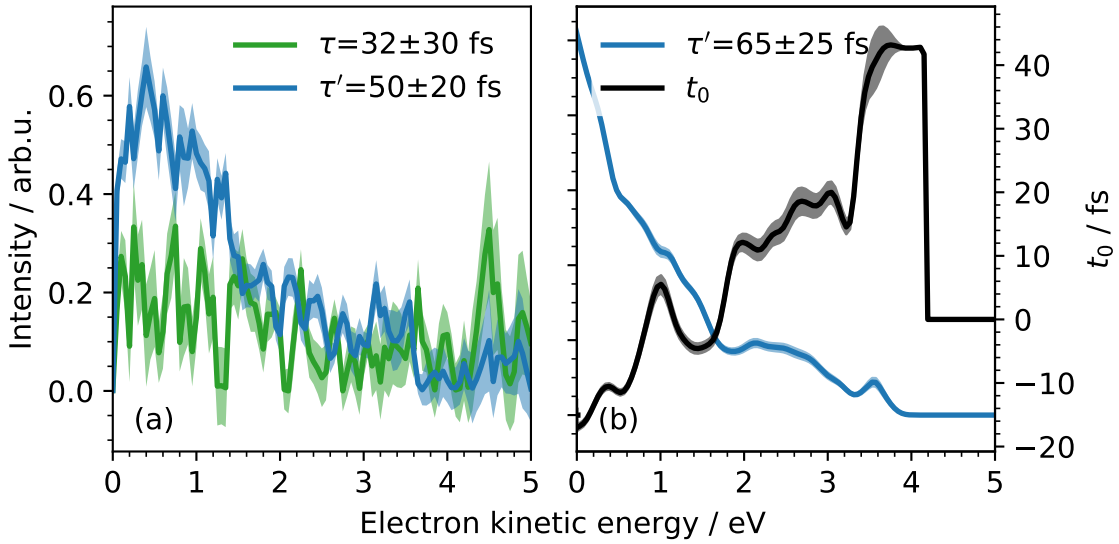

Figure S9: (a) Decay-associated spectra of the experimental TRPES and (b) simulated TRPES of AN. The experimental TRPES (a) was fitted with using a mono-exponential decay for the dynamics induced by both 200 nm (τ', blue) and 160 nm (τ , green). Uncertainties correspond to one standard deviation. Simulated TRPES (b) were fitted assuming a mono-exponential decay and a floating t_0, as described in[1]. Fitting both with the same mechanism was not possible, as the dynamics induced by 160 nm obscured the dynamics induced by 200 nm.

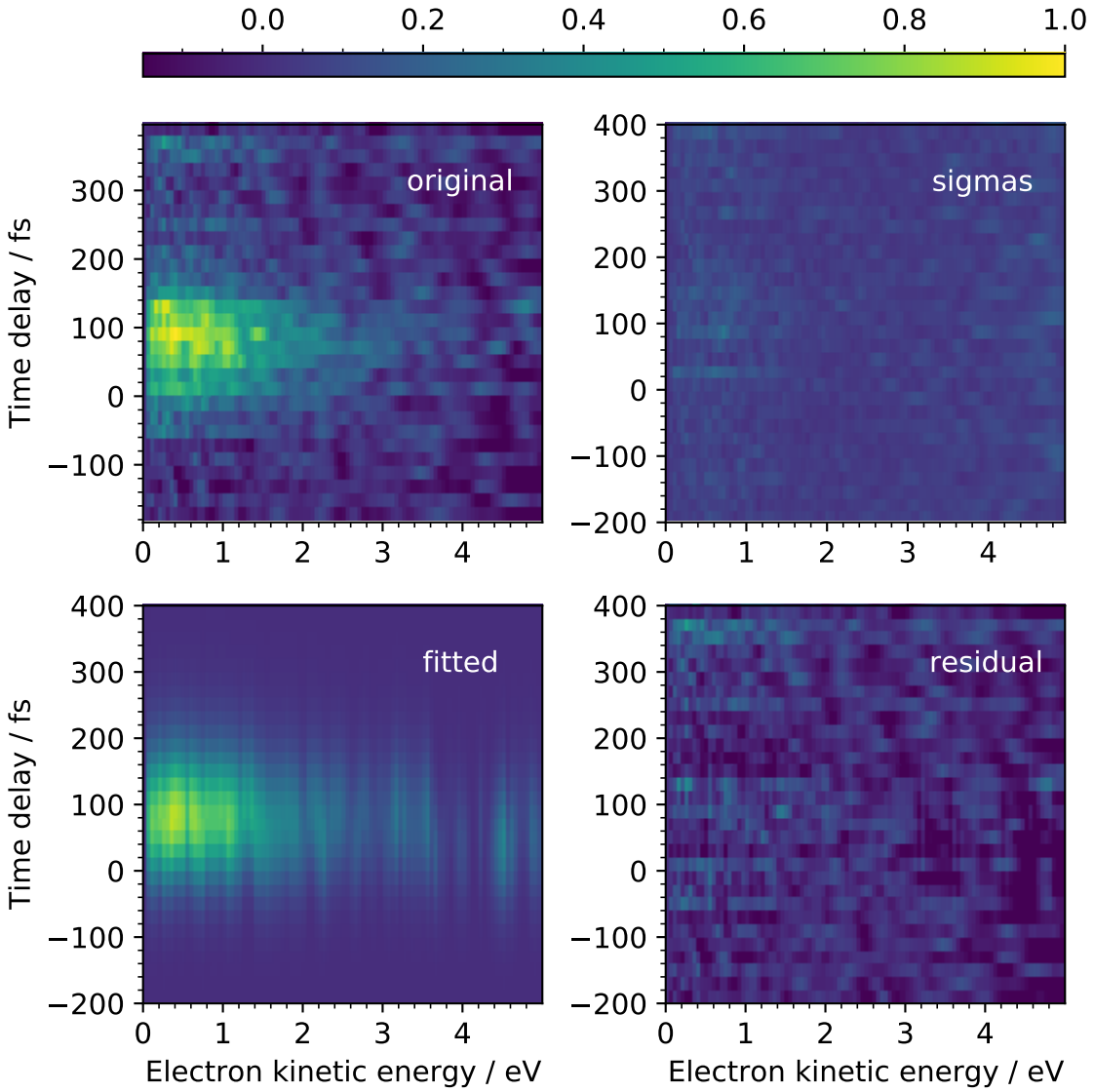

Figure S10: Experimental TRPES of AN (top left), experimental uncertainties of AN (top right), fit as described in Figure S9 (bottom left) and residuals between the experimental data and fit (bottom right).

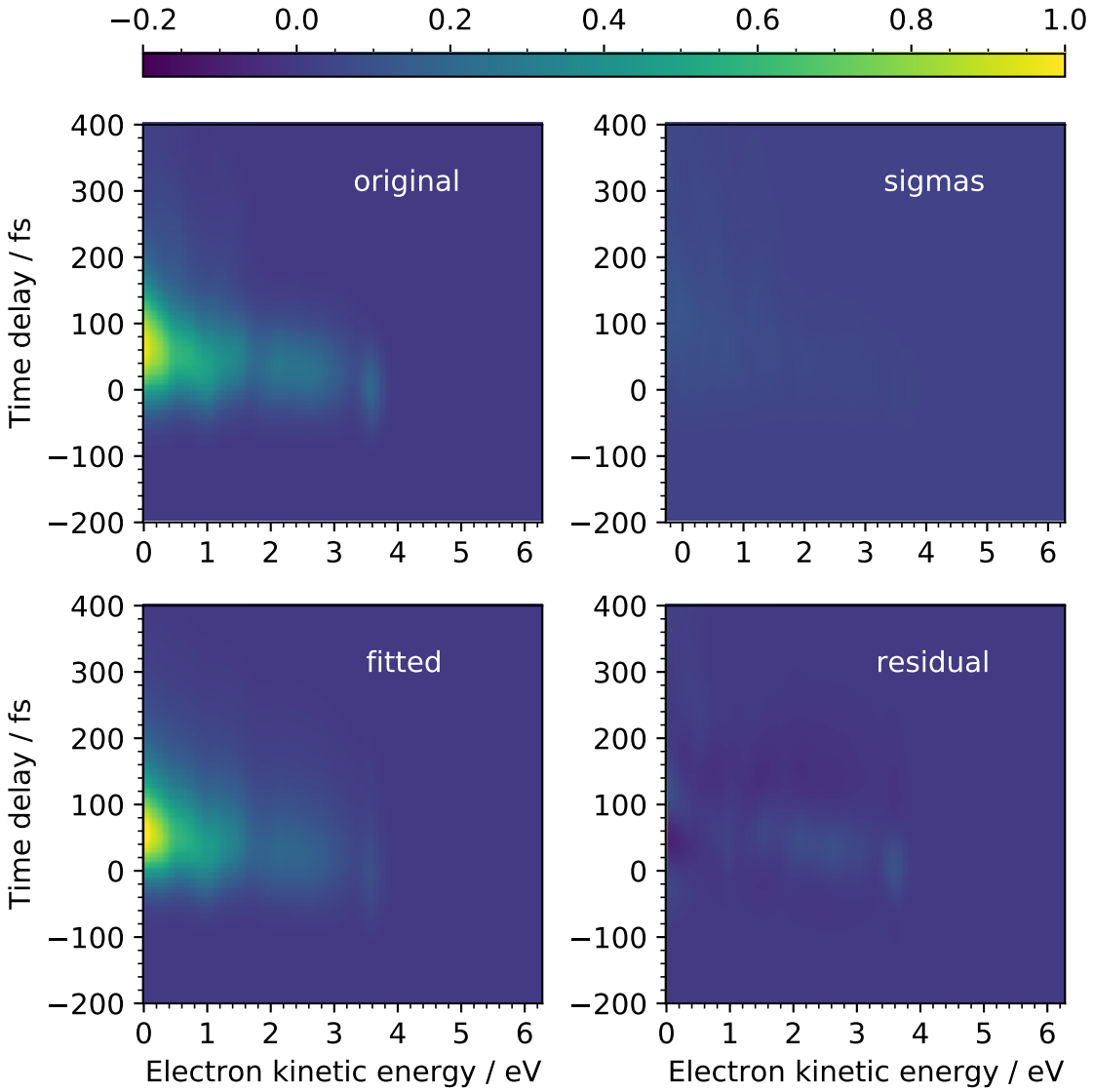

Figure S11: Simulated TRPES of AN (top left), uncertainties (top right), fit as described in Figure S9 (bottom left) and residuals between the simulated TRPES and fit (bottom right).

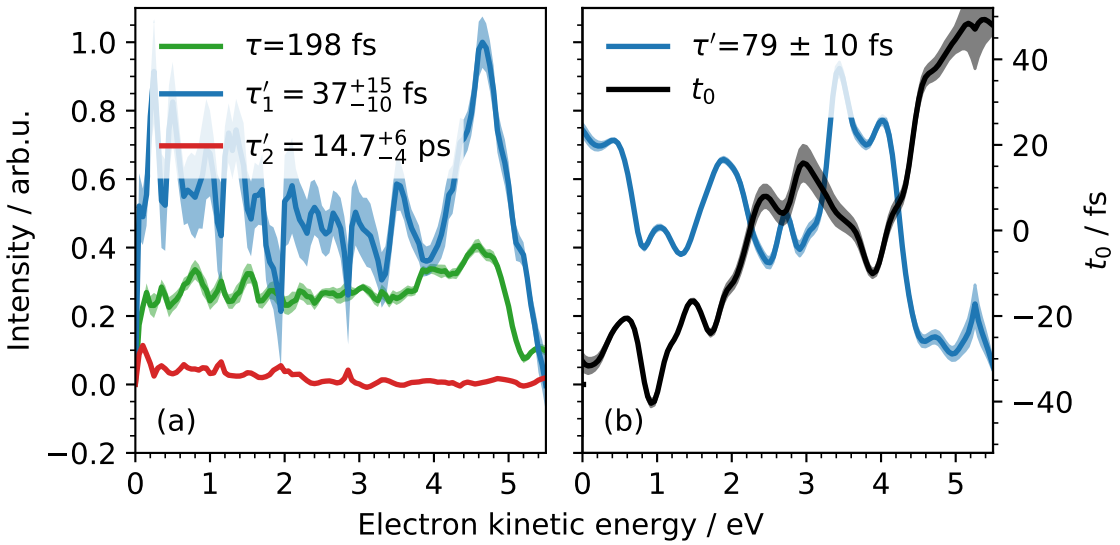

Figure S12: (a) Decay-associated spectra of the experimental TRPES and (b) simulated TRPES of MVE. The experimental TRPES (a) was fitted with using a mono-exponential decay for the dynamics induced by 160 nm (τ, green), determined independently from a 160 +266 nm experiment (see Figure S15), and a biexponential decay induced by 200 nm (τ_1', blue and τ_2', red). Uncertainties correspond to one standard deviation. Simulated TRPES (b) were fitted assuming a mono-exponential decay and a floating t_0, as described in [1].

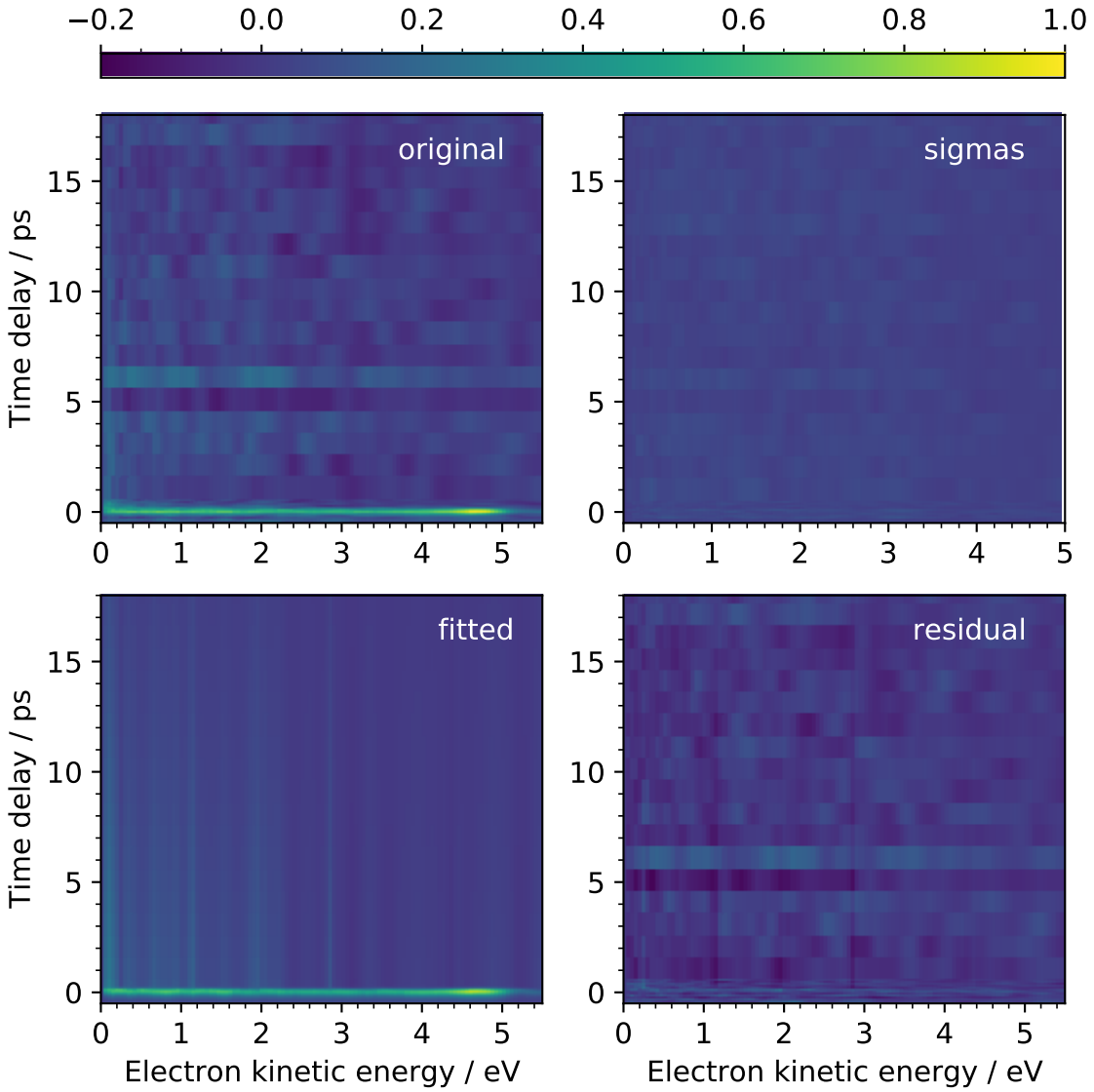

Figure S13: Experimental TRPES of MVE, 160 nm+200 nm (top left), sigmas (top right), fit according to the model described in Figure S12 (bottom left) and difference between the experimental TRPES and fit (bottom right).

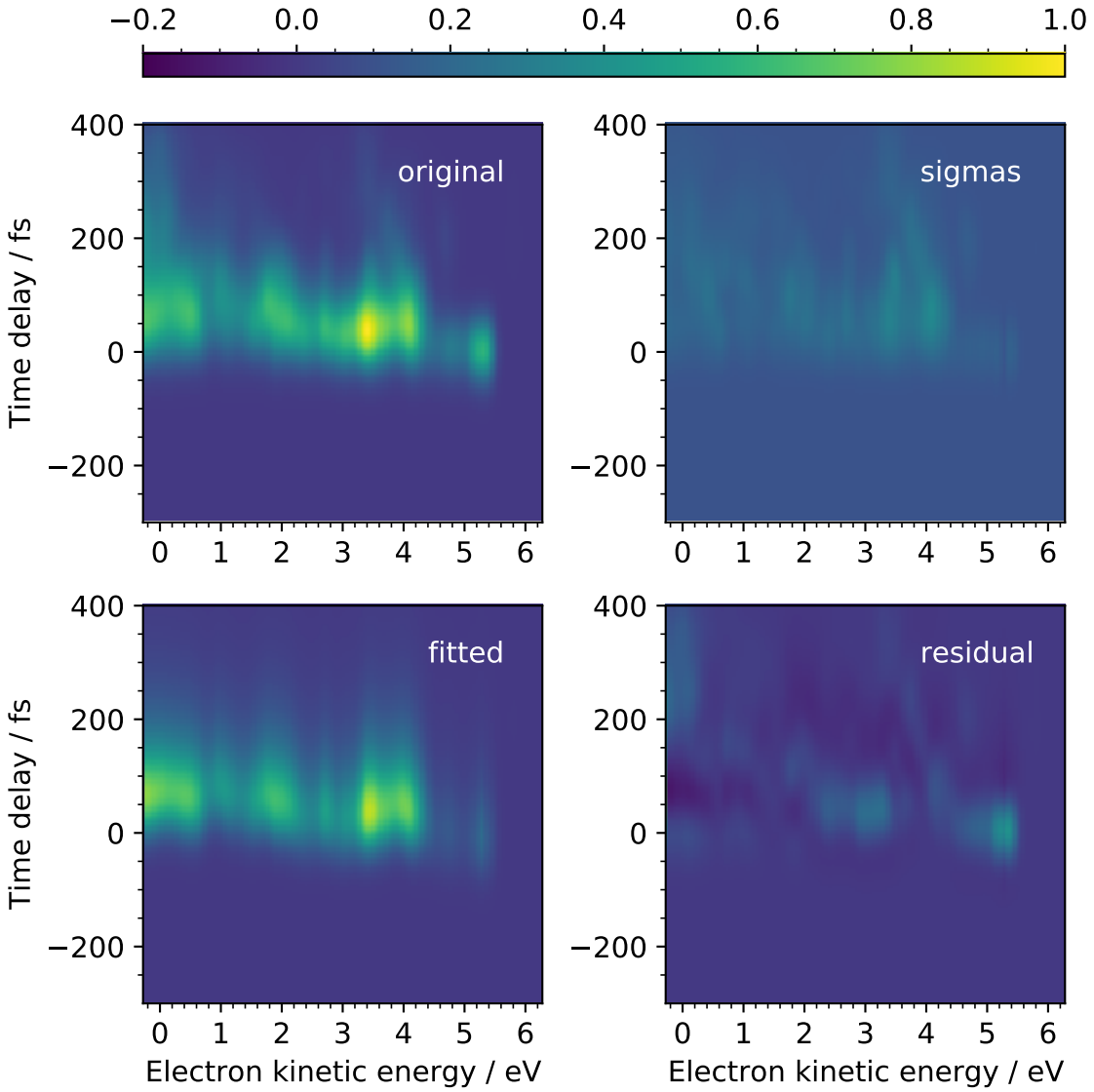

Figure S14: Simulated TRPES of MVE (top left), sigmas (top right), fit according to the model described in Figure S12 (bottom left) and difference between the simulated TRPES and fit (bottom right).

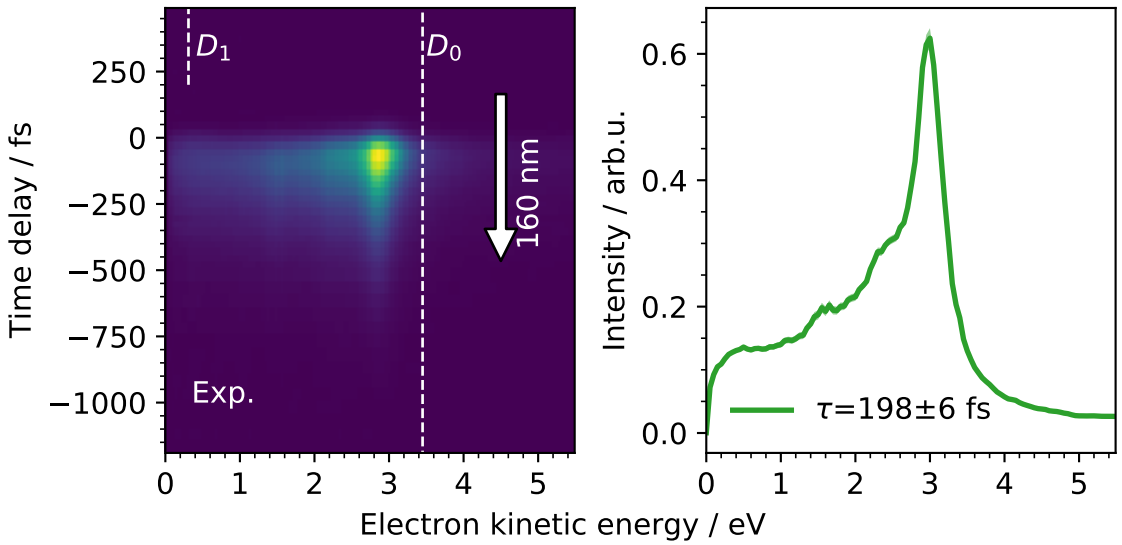

Figure S15: Experimental TRPES (left) for MVE with the corresponding DAS (right) in a 160 nm pump/266 nm probe experiment. The dotted lines corresponds the maximum kinetic photoelectron kinetic energies after ionization with 12.41 eV (266 nm and 160 nm) into D_0 (IE=8.96 eV^2) and D_1 (12.10 eV^2). The TRPES was fitted using a mono-exponential decay, and the extracted time-constant τ (green) was used in the fit of the 200/160 nm TRPES experiment (see Figure S12).

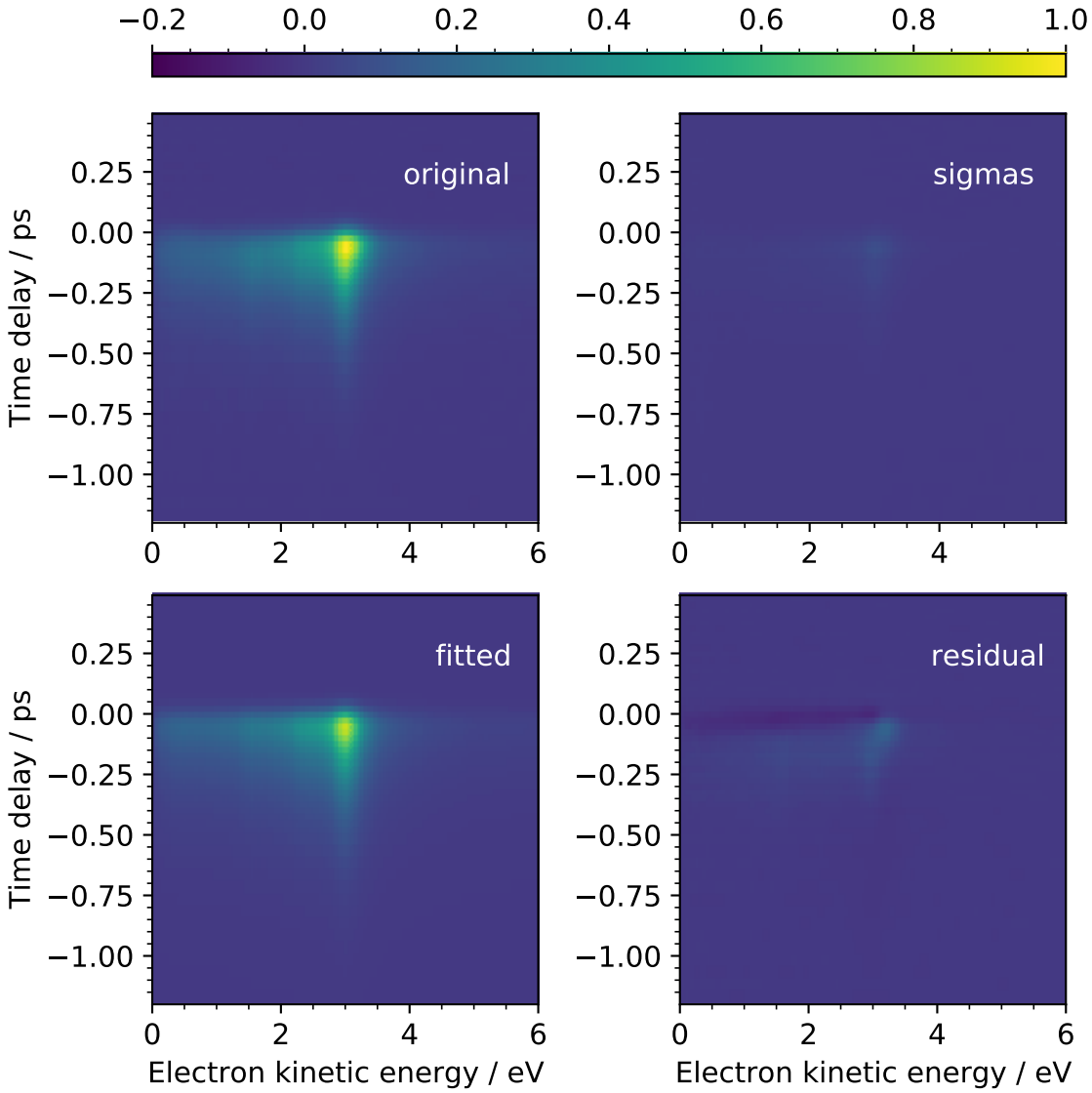

Figure S16: Experimental TRPES of MVE, 160 nm+266 nm (top left), sigmas (top right), fit according to the model described in Figure S15 (bottom left) and difference between the experimental TRPES and fit (bottom right).

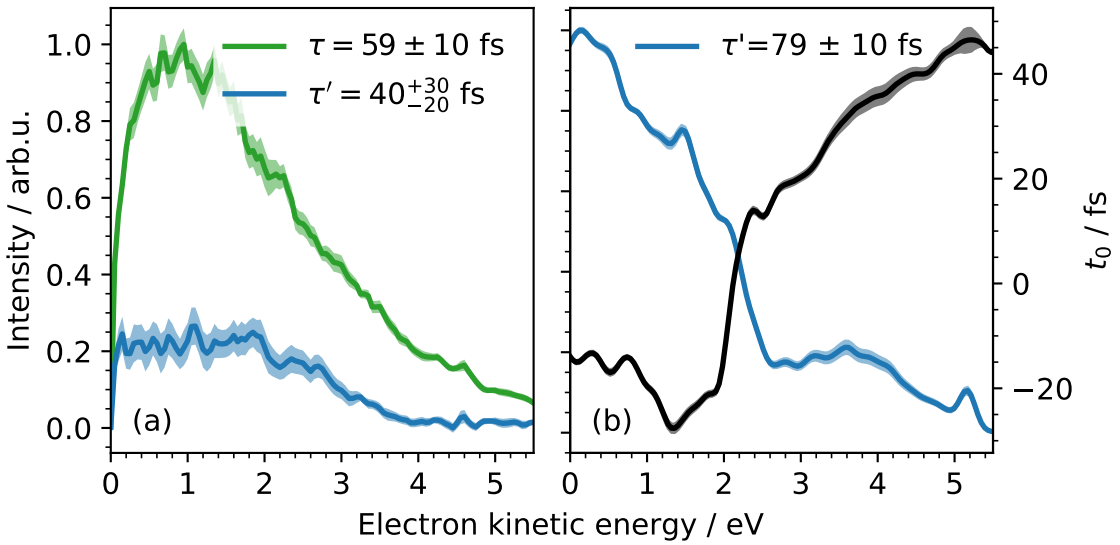

Figure S17: (a) Decay-associated spectra of the experimental TRPES and (b) theoretical TRPES of 1,2-MAN. The experimental TRPES (a) was fitted with using a mono-exponential decay for the dynamics induced by 160 nm (τ, green), determined independently from a 160 +266 nm experiment (see Figure S15), and a mono-exponential decay induced by 200 nm (τ', blue). Uncertainties correspond to one standard deviation. Simulated TRPES (b) were fitted assuming a mono-exponential decay and a floating t_0, as described in [1].

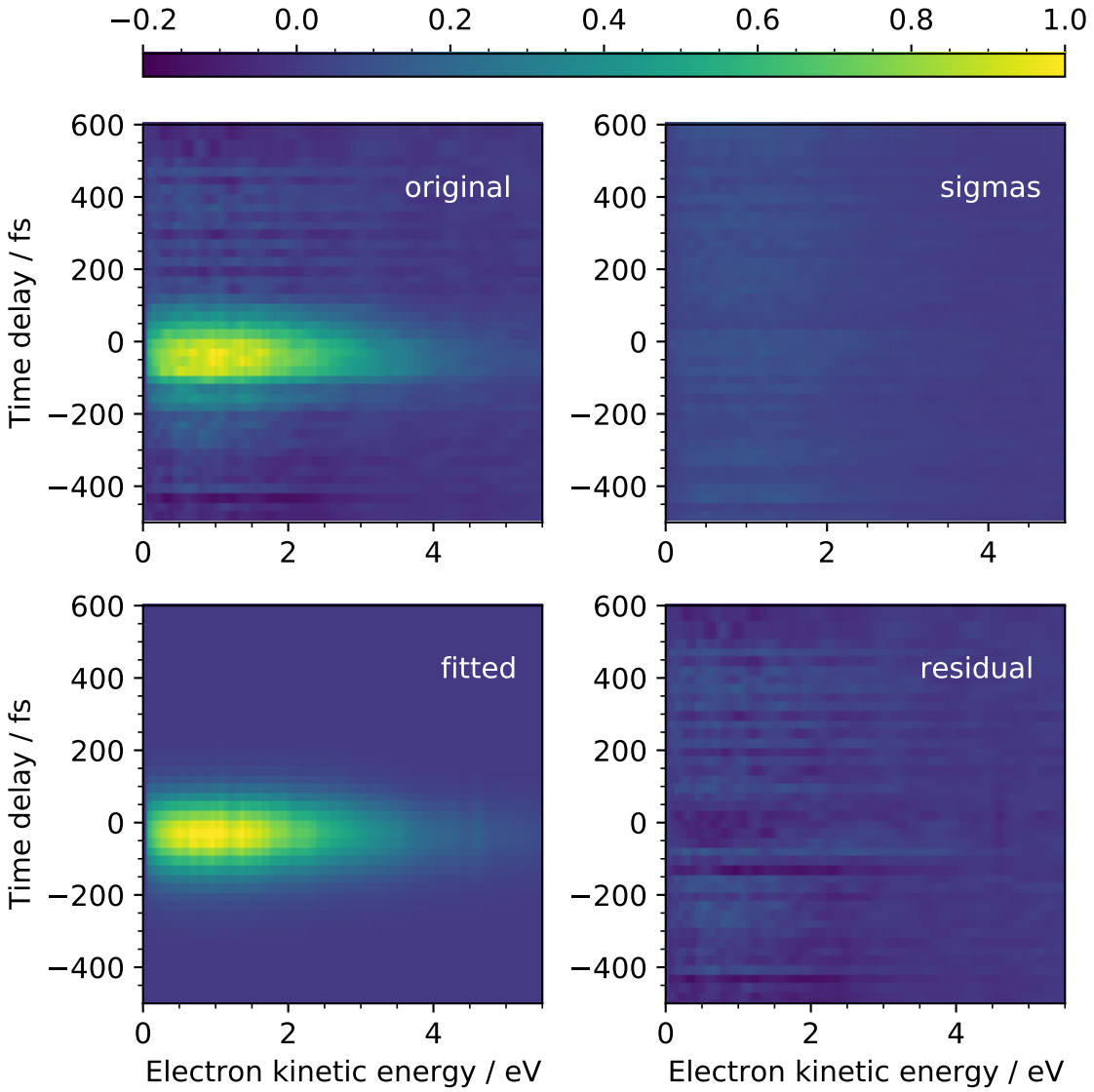

Figure S18: Experimental TRPES of 1,2-MAN (top left), sigmas (top right), fit according to the model described in Figure S17 (bottom left) and difference between the experimental TRPES and fit (bottom right).

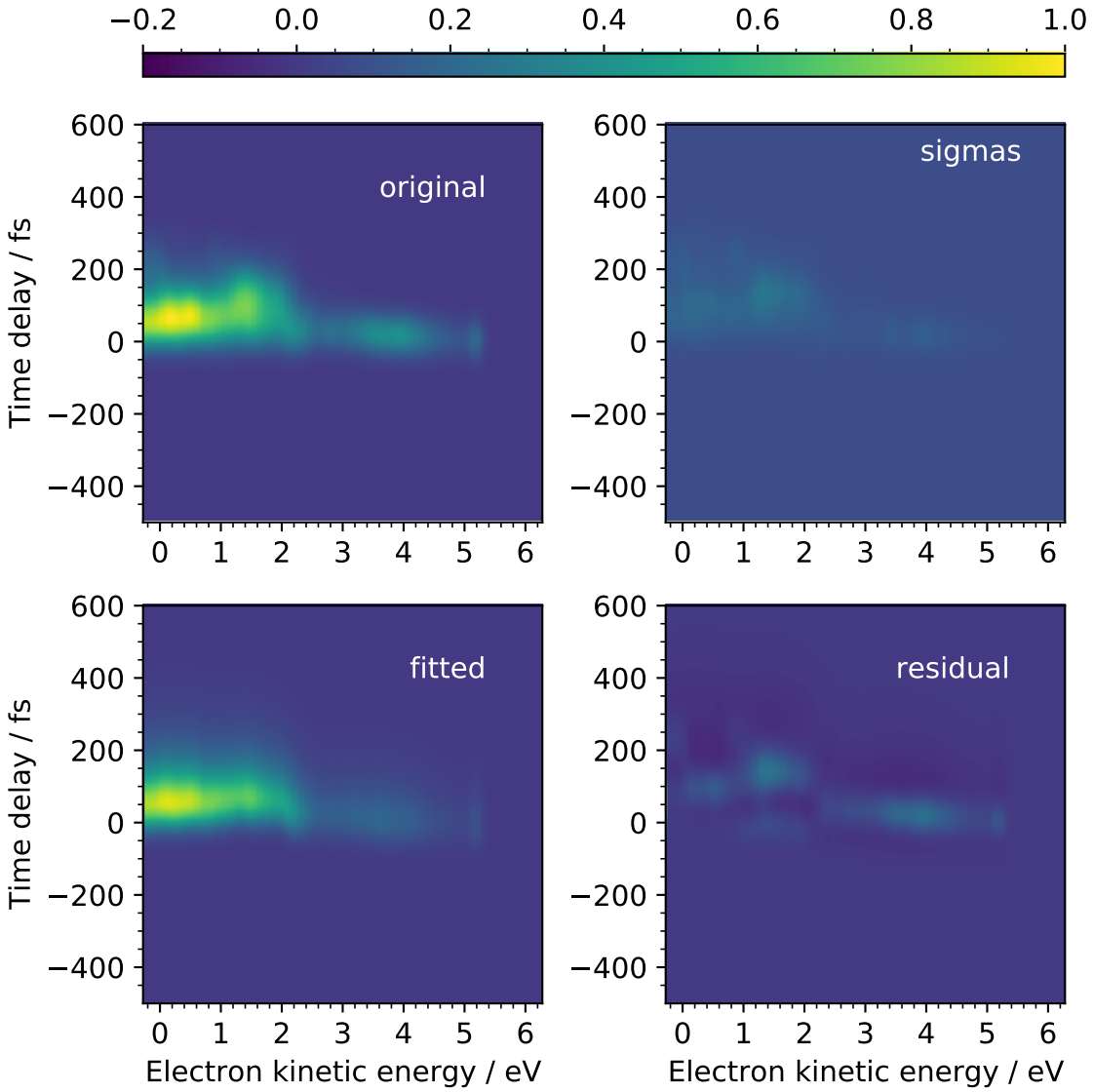

Figure S19: Simulated TRPES of 1,2-MAN (top left), sigmas (top right), fit according to the model described in Figure S17 (bottom left) and difference between the simulated TRPES and fit (bottom right).

References

(1) MacDonell, R. J.; Schalk, O.; Geng, T.; Thomas, R. D.; Feifel, R.; Hansson, T.; Schuurman, M. S. Excited state dynamics of acrylonitrile: Substituent effects at conical intersections interrogated via time-resolved photoelectron spectroscopy and ab initio simulation. *Journal of Chemical Physics* **2016**, *145*.

(2) Planckaert, A. A.; Doucet, J.; Sandorfy, C. Comparative study of the vacuum ultraviolet absorption and photoelectron spectra of some simple ethers and thioethers. *The Journal of Chemical Physics* **1974**, *60*, 4846–4853.